

Limits on thermal variations in a dozen quiescent neutron stars over a decade

Arash Bahramian^{1*}, Craig O. Heinke^{1,2}, Nathalie Degenaar³, Laura Chomiuk⁴, Rudy Wijnands⁵, Jay Strader⁴, Wynn C. G. Ho⁶, David Pooley^{7,8}

¹ *Dept. of Physics, CCIS 4-183, University of Alberta, Edmonton, AB T6G 2E1, Canada*

² *Humboldt Fellow, Max Planck Institut für Radioastronomie, Auf dem Hügel 69, 53121 Bonn, Germany*

³ *Institute of Astronomy, University of Cambridge, Madingley Road, Cambridge CB3 0HA, UK*

⁴ *Department of Physics and Astronomy, Michigan State University, East Lansing, MI 48824, USA*

⁵ *Anton Pannekoek Institute for Astronomy, University of Amsterdam, Postbus 94249, NL-1090 GE Amsterdam, The Netherlands*

⁶ *Mathematical Sciences and STAG Research Centre, University of Southampton, Southampton, SO17 1BJ, United Kingdom*

⁷ *Eureka Scientific, 2452 Delmer Street, Suite 100, Oakland, CA 94602-3017, USA*

⁸ *Sam Houston State University, Department of Physics, Farrington Building, Suite 204, Huntsville, Texas 77341, USA*

ABSTRACT

In quiescent low-mass X-ray binaries (qLMXBs) containing neutron stars, the origin of the thermal X-ray component may be either release of heat from the core of the neutron star, or continuing low-level accretion. In general, heat from the core should be stable on timescales $< 10^4$ years, while continuing accretion may produce variations on a range of timescales. While some quiescent neutron stars (e.g. Cen X-4, Aql X-1) have shown variations in their thermal components on a range of timescales, several others, particularly those in globular clusters with no detectable nonthermal hard X-rays (fit with a powerlaw), have shown no measurable variations. Here, we constrain the spectral variations of 12 low mass X-ray binaries in 3 globular clusters over ~ 10 years. We find no evidence of variations in 10 cases, with limits on temperature variations below 11% for the 7 qLMXBs without powerlaw components, and limits on variations below 20% for 3 other qLMXBs that do show non-thermal emission. However, in 2 qLMXBs showing powerlaw components in their spectra (NGC 6440 CX 1 & Terzan 5 CX 12) we find marginal evidence for a 10% decline in temperature, suggesting the presence of continuing low-level accretion. This work adds to the evidence that the thermal X-ray component in quiescent neutron stars without powerlaw components can be explained by heat deposited in the core during outbursts. Finally, we also investigate the correlation between hydrogen column density (N_H) and optical extinction (A_V) using our sample and current models of interstellar X-ray absorption, finding $N_H(\text{cm}^{-2}) = (2.81 \pm 0.13) \times 10^{21} A_V$.

Key words: accretion, accretion discs, binaries: close, stars: neutron, X-rays: binaries, globular clusters: individual: Terzan 5; NGC 6440; NGC 6266

1 INTRODUCTION

Transient low-mass X-ray binaries (LMXBs) show occasional outbursts, separated by periods of quiescence (typically months to years) in which their X-ray emission dramatically drops, to $L_X = 10^{31}\text{--}10^{33}$ erg s^{−1}, and there is little or no accretion occurring. The X-ray spectra of quiescent LMXBs (qLMXBs) containing a neutron star (NS) consist of a soft blackbody-like component (if fit with a blackbody, giv-

ing typical temperatures of 0.2–0.3 keV) and sometimes an additional harder component, typically fit with a powerlaw, with photon-index between 1 and 2 (e.g. Campana et al. 1998; Rutledge et al. 1999). The origin of the powerlaw component in these systems may be continuing low level accretion onto the NS, an accretion shock between infalling matter and the NS’s magnetosphere or a pulsar wind, or synchrotron radiation from a pulsar wind nebula (e.g. Campana et al. 1998; Bogdanov, Grindlay & van den Berg 2005). Recent X-ray observations support boundary-layer emission from accretion onto the NS as the likely origin of

* E-mail: bahramia@ualberta.ca

the hard powerlaw component at least in some sources (e.g. Cen X-4 and PSR J1023+0038, Chakrabarty et al. 2014; D’Angelo et al. 2015; Archibald et al. 2014; Wijnands et al. 2014).

The blackbody-like component can be well-described by NS hydrogen atmosphere models, with an implied radius consistent with theoretically predicted NS radii (e.g. Rajagopal & Romani 1996; Zavlin, Pavlov & Shibano 1996; Rutledge et al. 1999, 2001). The soft component has been widely interpreted as the slow (10^4 years) release of heat from the core of the NS, deposited through deep crustal heating during previous episodes of accretion (Brown, Bildsten & Rutledge 1998). A nearly identical soft spectrum can also be created in the upper layers of the NS atmosphere by low-level accretion (Zampieri et al. 1995; Zane, Turolla & Treves 2000), though the most detailed model predicts, in addition, an optically thin high-temperature bremsstrahlung component (Deufel, Dullemond & Spruit 2001), which may be identified with the powerlaw component (e.g. Bahramian et al. 2014). However, low-level accretion at sufficiently high rates (corresponding to $L \sim 10^{33}$ erg/s) could maintain metals in the atmosphere at abundances sufficient to soften the spectrum, leading to an overestimate of R (Rutledge et al. 2002b). The question of the origin of the thermal component in qLMXBs is of intense interest, since fitting the thermal spectra of qLMXBs in globular clusters is often used to measure the radius of NSs and place constraints on the dense matter equation of state (Rutledge et al. 2002a; Heinke et al. 2006a; Webb & Barret 2007; Steiner, Lattimer & Brown 2010, 2013; Guillot, Rutledge & Brown 2011; Servillat et al. 2012; Guillot et al. 2013; Guillot & Rutledge 2014; Lattimer & Steiner 2014; Heinke et al. 2014; Özel et al. 2015; see also Miller et al. 2013). Confirmation that thermal spectra of qLMXBs (especially those without powerlaw components) are not produced by accretion would eliminate the possibility that metals remain in the atmosphere, and thus eliminate a systematic uncertainty in this method of constraining the NS radius.

At low accretion rates, the NS’s magnetic field is expected to exercise a propeller effect, which retards the accretion of material onto the NS surface (Illarionov & Sunyaev 1975). The mechanism is that ionized disc material will become attached to the magnetic field lines when the magnetospheric pressure exceeds the gas pressure; if this boundary (the edge of the magnetosphere) occurs at a radius larger than the corotation radius, the material is accelerated to velocities higher than the Keplerian orbital velocity, throwing it away, and possibly out of the system. On the other hand, simulations of low-level accretion onto a magnetic propeller predict some material will reach the neutron star (Romanova et al. 2002; Kulkarni & Romanova 2008; D’Angelo & Spruit 2010, 2012). Pulsations have recently been identified from two (relatively bright) qLMXBs, the transitional pulsars PSR J1023+0038 at $L_X = 3 \times 10^{33}$ erg/s, and XSS J12270-4859 at $L_X = 5 \times 10^{33}$ erg/s, proving that matter accretes onto the surface even though it seems to be in the propeller regime (Archibald et al. 2014; Papitto et al. 2014). Detections of pulsations at low accre-

tion rates from X-ray pulsars (with known magnetic fields) in high-mass X-ray binaries also suggest continued accretion in the propeller regime (e.g. Negueruela et al. 2000; Reig, Doroshenko & Zezas 2014). Note that pulsations have not yet been detected from quiescent LMXBs other than transitional MSPs (D’Angelo et al. 2015; Elshamouty et al., in prep.).

Thus, there is evidence that continued accretion can produce an X-ray spectrum consistent with the soft component in qLMXBs, by heating the NS surface (Zampieri et al. 1995; Zane, Turolla & Treves 2000; Deufel, Dullemond & Spruit 2001) and that continued accretion can continue at very low accretion rates. Testing for variability is a promising method to constrain whether thermal emission from qLMXBs is driven by accretion. X-ray emission driven by heat emerging from the core should be stable on timescales $\sim 10^4$ years (Colpi et al. 2001; Wijnands, Degenaar & Page 2013). For NSs that have undergone recent episodes of accretion, decays of the thermal component are seen (e.g. Wijnands et al. 2002; Cackett et al. 2008; Degenaar et al. 2011; Fridriksson et al. 2011), attributed to heat leaking from shallower levels in the crust, where it was deposited during the outburst (Ushomirsky & Rutledge 2001; Rutledge et al. 2002c). This variation should be a monotonic decline on a time scale of years/decades. Possibilities for variations of the thermal component without accretion, based on changes in the chemical composition of the envelope, have been advanced (Brown, Bildsten & Chang 2002; Chang & Bildsten 2004), but these do not predict significant changes on timescales of years without intervening outbursts. Alternatively, if the thermal component is caused by continuous accretion onto a NS, the temperature may vary in either direction, on a range of timescales.

Strong evidence for variability of the thermal component of some qLMXBs during quiescence has been reported for the transients Aquila X-1 (Rutledge et al. 2002b; Cackett et al. 2011), Cen X-4 (Campana et al. 1997, 2004; Cackett et al. 2010), XTE J1701-462 (Fridriksson et al. 2010), and MAXI J0556-332 (Homan et al. 2014). Each of the transient qLMXBs that showed strong variation in the thermal component also showed a relatively strong powerlaw component, typically making up $\sim 50\%$ of the 0.5-10 keV flux (e.g. Rutledge et al. 2002b; Cackett et al. 2010; Homan et al. 2014). So far, this is consistent with the suggestion (Heinke et al. 2003d) that continued accretion is responsible for both the powerlaw component (at least for $L_X \gtrsim 10^{33}$ erg/s, Jonker et al. 2004) and variability.

Globular clusters (GCs) are highly efficient factories for producing X-ray sources (~ 100 times more efficient than the rest of the Galaxy, per unit mass; Katz 1975; Clark 1975). The densest and most massive globular clusters have been shown by Chandra to contain multiple soft X-ray sources with L_X in the 10^{32} – 10^{33} erg/s range, whose spectra strongly indicate that they are qLMXBs (Grindlay et al. 2001; Pooley et al. 2002; Heinke et al. 2003a,b; Pooley et al. 2003; Maxwell et al. 2012). These can be discriminated from other sources (spectrally harder cataclysmic variables, chromospherically active binaries, and millisecond radio pulsars) through spectral fitting (e.g. Rutledge et al. 2002a),

or through X-ray colours and luminosities (Heinke et al. 2003d; Pooley & Hut 2006). The majority of the candidate qLMXBs show no evidence for powerlaw components in their spectra (Heinke et al. 2003d). This may be a selection effect, since it is easier to discriminate qLMXBs from other sources if they show purely thermal spectra. Deep Chandra observations of globular clusters identify a significant population of candidate qLMXBs with strong powerlaw components, which require high-quality X-ray spectra to confidently identify the thermal components (Heinke, Grindlay & Edmonds 2005), and half of the transient cluster LMXBs followed up with Chandra are too faint, or too dominated by a powerlaw component, for detection of a thermal component (e.g. Wijnands et al. 2005; Heinke et al. 2010; Linares et al. 2014).

Several qLMXBs in globular clusters with thermal components have been examined to search for variations between observations. Several show flux variations, but spectral analyses have permitted these variations to be driven only by changes in the normalization of the powerlaw component (Heinke, Grindlay & Edmonds 2005; Cackett et al. 2005; Bahramian et al. 2014), or of obscuring material—the latter especially in edge-on systems (e.g. Nowak, Heinz & Begelman 2002; Heinke et al. 2003c; Wijnands et al. 2003). A few qLMXBs without detectable powerlaw components have repeated deep observations with *Chandra*, permitting sensitive measurements for variability; these include (with 90% confidence variability limits) 47 Tuc X7, $\Delta T/T < 1.0\%$ over 2 years (Heinke et al. 2006a); NGC 6397 U18, $\Delta T/T < 1.4\%$ over 10 years (Guillot, Rutledge & Brown 2011; Heinke et al. 2014); M28 source 26 (no variation found, Servillat et al. 2012) and ω Cen, $\Delta T/T < 2.1\%$ over 12 years (Heinke et al. 2014).

We are interested in whether this lack of variability is the norm in thermal components of globular cluster qLMXBs, and whether (if it is observed anywhere) there is a correlation with the presence of powerlaw components. Strong evidence that globular cluster qLMXBs without powerlaw components are not variable would increase confidence in the assumptions used to derive radius measurements for their NSs and obtain constraints on the dense matter equation of state. We choose to focus on qLMXBs in globular clusters, since globular clusters are the only places where we can find and study large populations of qLMXBs in single Chandra pointings (and with relatively low optical extinction, compared to many qLMXBs in the Galactic Plane) and distances to qLMXBs in globular clusters are known better than to the ones in the field.

In this paper, we analyze a sample of 12 qLMXBs in 3 globular clusters, NGC 6266 (M 62), NGC 6440, and Terzan 5, searching for variations over multiple observations spanning roughly a decade. Each of these dense globular clusters have at least 4 candidate qLMXBs, and multiple *Chandra*/*ACIS* observations. When this work was in an advanced state, Walsh, Cackett & Bernardini (2015) reported on the analysis of 9 similar sources in Terzan 5 and NGC 6440 as considered here, though using fewer Terzan 5 observations, and not including NGC 6266. We directly compare our results with those of Walsh et al., finding general agreement. In §2, we describe our data reduction and analysis methods.

In §3, we show the results of our analysis, and in §4, we discuss the implications.

2 DATA REDUCTION AND ANALYSIS

All datasets were obtained using ACIS-S in Faint, Timed Exposure mode. The data covers a time span of 9 to 12 years for the GCs in our sample (Table 1). We used CIAO 4.6 (Fruscione et al. 2006) and CALDB 4.6.2 for data re-processing following standard CIAO science threads¹. We chose known (and candidate) LMXBs with more than ~ 60 photons (per epoch) for spectral analysis, resulting in a total sample of 12 sources. These targets are tabulated in Table 2. We performed spectral extraction using the task *specextract* and performed spectral analysis in the 0.3–10 keV energy range using HEASOFT 6.16 and XSPEC 12.8.2 (Arnaud 1996). We combined (using the CIAO *dmmerge* tool) spectra from observations which occurred within a month for our targets in Terzan 5, to improve the spectral quality. We grouped each spectrum by 15 counts per bin, and used chi-squared statistics for analysis. Details of the spectral extractions and analyses for each cluster are discussed in §3. All uncertainties reported in this paper are 90% confidence.

We fit the spectra with an absorbed neutron star atmosphere, plus a powerlaw (if needed). We used the NSATMOS (Heinke et al. 2006a) NS atmosphere model, with the NS mass and radius frozen to the canonical values of $1.4 M_\odot$ and 10 km, the normalization fixed to 1 (implying radiation from the entire surface), and the distance fixed to the estimated distance of the cluster (see §3). In cases where this single-component model does not produce a good fit, leaving significant residuals at high energies (≥ 3 keV), a powerlaw component (PEGPWRLW, with normalization set to represent flux in the 0.5–10 keV range) was added to the model. In cases where it was unclear whether the fit was improved by adding a second component, we checked this by an F-test. We set the powerlaw photon index (Γ) as a free parameter when fitting datasets where the data quality above 3 keV is high enough to constrain this quantity. However, in datasets where the data quality is not sufficient to do this, we fixed the photon index to 1.5, which is a typical value from LMXBs in quiescence (Campana et al. 1998, 2004; Fridriksson et al. 2011; Degenaar et al. 2011; Chakrabarty et al. 2014).

We fit all spectra available for each source simultaneously. We tied the N_H and powerlaw photon index to a single value for each source, and let the NS temperature and powerlaw flux vary between observations. There is good evidence that N_H does not vary during the spectral evolution of most LMXBs (Miller, Cackett & Reis 2009). Although correlated variations in N_H and powerlaw photon index have been proposed to explain spectral variability in Aql X-1 in quiescence (Campana & Stella 2003), such a model requires the powerlaw to dominate over the thermal component of the spectrum, and forces the photon index to (unreasonably) high values (≥ 2.5). Fitting individual high-quality spectra of Aql X-1 (Cackett et al. 2011),

¹ <http://cxc.harvard.edu/ciao/threads/index.html>

SAX J1808.4-3658 (Heinke et al. 2009), and Terzan 5 X-3 (Bahramian et al. 2014) in quiescence gives consistent values (within the errors) between epochs for both N_H and the powerlaw photon index. Deep observations of Cen X-4 do show evidence for powerlaw photon index changes (Cackett et al. 2010), changing from ~ 1.7 in all observations where $L_X < 2 \times 10^{32}$ erg/s, to ~ 1.4 at higher L_X values (Chakrabarty et al. 2014). Fridriksson et al. (2010) also find evidence for variation in the powerlaw photon index in XTE J1701-462, but only when L_X reaches $> 2 \times 10^{34}$ erg/s, well above the range discussed here. Summarizing these observations, when the total L_X does not vary by a large factor, the powerlaw photon index appears to remain roughly constant. As we will see below, our observations do not reveal large swings in L_X , so we feel that keeping a fixed powerlaw index is justified.

As we are looking for relative variations in kT , to estimate the uncertainties in the NS temperature and powerlaw flux, after initially fitting the N_H we then froze N_H to its best-fit value. In cases where the source shows significantly higher N_H value than the average of the cluster, we investigated the possibility of intrinsic absorption leading to variations in N_H (§3).

We also search for signs of temporal variations during each observation for all sources. (Due to the limited signal, we explore only total flux variations.) We extracted background-subtracted lightcurves in 0.3-7 keV band for each source using CIAO task *dmextract*. Due to the faint nature of the sources in our study, we binned each lightcurve by 1000 s. We used the FTools task *lcstats* to perform chi-squared and Kolmogorov-Smirnov (KS) tests for variations. Since we ran these tests on 80 lightcurves (all sources in our sample in all observations used²), we require a false-alarm probability below $5\%/80=0.06\%$ to identify variability at 95% confidence (Note that null-results from a test do not prove the source did not vary).

3 RESULTS

3.1 Hydrogen column density

We constrained the hydrogen column density (N_H) for each GC using our sample of LMXBs. In our primary analysis in this paper, we forced the N_H to a single value for all observations of each source. We used the Tuebingen-Boulder ISM absorption model (TBABS) with Wilms, Allen & McCray (2000) abundances and Balucinska-Church & McCammon (1992) cross sections. (We tested the Verner et al. (1996) cross sections, and found no difference in our results). We also tried using the abundances of Anders & Grevesse (1989) for comparison (see below). After constraining N_H values for each target, we calculated the mean value for sources in each cluster. (We excluded Terzan 5 CX 9 from this analysis due to possible intrinsic absorption—see §3.4.) We compare these values with those produced by adopting reddening values,

E(B-V), from the Harris catalog (Harris 1996, 2010 revision) and the relation between N_H and optical extinction (A_V) from Güver & Özel (2009):

$$N_H(\text{cm}^{-2}) = (2.21 \pm 0.09) \times 10^{21} A_V \quad (1)$$

(Table 3). The N_H values calculated from A_V using the relation of Güver & Özel (2009) agree nicely with fits to the X-ray spectra using the Anders & Grevesse (1989) abundances—which makes sense, as Güver & Özel (2009) used N_H estimates from the literature on X-ray studies of supernova remnants, most of which used Anders & Grevesse (1989) abundances. However, N_H values measured from spectral fitting using Wilms, Allen & McCray (2000) abundances are $\sim 27\%$ higher than predicted using Güver & Özel (2009). This makes sense, because the Wilms, Allen & McCray (2000) abundances are typically $\sim 30\%$ lower for X-ray relevant elements. We therefore introduce a new relation between N_H and A_V , designed specifically for use with the Wilms, Allen & McCray (2000) abundances,

$$N_H(\text{cm}^{-2}) = (2.81 \pm 0.13) \times 10^{21} A_V \quad (2)$$

where the error is the $1\text{-}\sigma$ scatter we measure in the relation from the fit. We derived this equation from fitting a linear model to N_H values measured for 11 out of 12 sources in our sample (we excluded Terzan 5 CX 9 due to possible presence of enhanced absorption). We also investigated the effects of including dust scattering for point sources by adding a scattering model (Predehl et al. 2003) to our spectral model, with A_V fixed to $0.117 \times N_H / (10^{22} \text{ cm}^{-2})$. We found that dust scattering causes a slight decrease of $\approx 1\%$ in the N_H values, and thus increases the A_V -to- N_H conversion factor to $2.84 \times 10^{21} \text{ cm}^{-2}$. As this work was being finalized, Foight et al. (2015) published their investigation of the A_V -to- N_H correlation using optical vs. X-ray studies of supernova remnants, also using Wilms, Allen & McCray (2000) abundances, which found the conversion factor to be $2.87 \pm 0.12 \times 10^{21} \text{ cm}^{-2}$. This is in complete agreement with our results.

3.2 NGC 6266

NGC 6266 (M 62) is a massive dense globular cluster. At least 26 X-ray sources can be identified in *Chandra* images of the cluster, of which 5 have been suggested to be qLMXBs on the basis of their soft spectra and X-ray luminosities (Pooley et al. 2003; Heinke et al. 2003d). One of these (the brightest, and with the hardest X-ray spectrum; reasonably fit by an absorbed powerlaw of photon index 2.5 ± 0.1) shows strong evidence (from its radio/X-ray flux ratio) for containing a black hole (Chomiuk et al. 2013). We use two deep *Chandra*/ACIS observations (Table 1) to study the other 4 soft candidate qLMXBs, which we name CX 4, CX 5, CX 6, and CX 16 (ordering the detected sources by *Chandra* countrates). In the 2002 observation, the cluster core is 2.5 arcminutes off-axis, and the sources have visibly elongated point-spread functions. To address this issue, we used elliptical extraction regions of the same size for all sources. The 2014 observation was performed on-axis, so we used circular extraction regions. We show images of these observations

² We excluded one of Terzan 5 observations (Obs.ID 13705) from this investigation due to its short exposure (14 ks).

Target	Obs. ID	Date	Exposure (ks)
NGC 6266	02677	2002-05-12	62
	15761	2014-05-05	82
NGC 6440	00947	2000-07-04	23
	03799	2003-06-27	24
	10060	2009-07-28	49
Terzan 5	03798	2003-07-13	40
	10059	2009-07-15	36
	13225	2011-02-17	30
	13252	2011-04-29	40
	13705	2011-09-05	14 ^A
	14339	2011-09-08	34 ^A
	13706	2012-05-13	46
	14475	2012-09-17	30
	14476	2012-10-28	29
	14477	2013-02-05	29 ^B
	14625	2013-02-22	49 ^B
	15615	2013-02-23	84 ^B
	14478	2013-07-16	29
	14479	2014-07-15	29 ^C
	16638	2014-07-17	72 ^C
	15750	2014-07-20	23 ^C

Table 1. Chandra ACIS observations used in this study. A, B, C: We merged spectra extracted from all observations marked A (and merged those marked B, etc.), as they occurred close in time.

Source	CXOGlb J	L_X ($10^{32} \text{erg s}^{-1}$, 0.5-10 keV)
NGC 6266 CX4	170113.09–300655.43	4.5±0.3
NGC 6266 CX5	170113.10–300642.33	4.2±0.3
NGC 6266 CX6	170113.76–300632.48	3.9±0.3
NGC 6266 CX16	170112.58–300622.38	1.0±0.2
NGC 6440 CX1	–	10±1
NGC 6440 CX2	–	14±1
NGC 6440 CX3	–	8±1
NGC 6440 CX5	–	7.4±0.8
Terzan 5 CX9	174804.8–244644	9.0±0.9
Terzan 5 CX12	174806.2–244642	7.0±0.8
Terzan 5 CX18	174805.2–244651	6.3±0.6
Terzan 5 CX21	174804.2–244625	4.4±0.5

Table 2. Candidate LMXBs studied in this paper. Luminosities are based on latest epoch used for each GC and are measured in this study. Reported uncertainties for luminosities are 90% confidence and do not include uncertainties in distance. References for source identification: This work (NGC 6266), Pooley et al. 2002 (NGC 6440), (3) Heinke et al. 2006b (Terzan 5).

and extraction regions in Fig. 1. We ran *wavdetect* to determine accurate positions and brightnesses of these X-ray sources, and corrected the astrometry by applying coordinate shifts to match the radio and X-ray positions of M62 CX1.

We assumed a distance of 6.8 kpc, and a reddening of $E(B-V)=0.47$ mag, for NGC 6266 in our analysis (Harris 1996, 2010 revision). Assuming $R_V=3.1$, this reddening gives $A_V=1.46$ mag. The A_V/N_H relation of Güver & Özel (2009) which is based on Anders & Grevesse (1989) abundances, predicts $N_H=3.2 \times 10^{21} \text{ cm}^{-2}$ for this cluster based on Anders & Grevesse (1989) abundances; in

§3.1, we use N_H values measured from our spectral analysis of X-ray observations to derive a new relationship between N_H and A_V , $N_H=2.8 \times 10^{21} A_V$, specifically for use with the Wilms, Allen & McCray (2000) abundances.

Due to the relatively low interstellar absorption and reasonable fluxes of our targets, the spectra from this cluster are of high quality (Fig. 2, top left). We found no evidence of temperature variations in these objects (Table 4). For three of our targets (CX4, CX5 & CX6) we constrain temperature variations to less than 5%. For CX16 this limit is < 10% due to its faintness.

NGC 6266 CX4 is the only candidate qLMXB in NGC

GC	E(B-V) (mag)	A _V (mag)	Calculated N _H (Guver09) ($\times 10^{21}$ cm ⁻²)	Measured N _H (Anders89) ($\times 10^{21}$ cm ⁻²)	Measured N _H (Wilms00) ($\times 10^{21}$ cm ⁻²)	Discrepancy (%)
NGC 6266	0.47	1.46	3.2 \pm 0.2	3.2 \pm 0.4	4.1 \pm 0.4	22 \pm 9
NGC 6440	1.07	3.32	7.3 \pm 0.5	7.2 \pm 0.6	10 \pm 1	27 \pm 9
Terzan 5	2.61	8.09	18 \pm 1	17 \pm 2	26 \pm 2	31 \pm 9

Table 3. Comparing N_H for GCs based on different assumptions. Calculated N_H is calculated based on relation between A_V and N_H provided by Güver & Özel (2009). The uncertainties reported for calculated N_H values based on Güver & Özel (2009) are only statistical uncertainties from the correlation. Measured N_H values are based on X-ray spectroscopy of the sources in our sample (average and uncertainty calculated for each GC; see text) with two different assumptions for the abundances of elements (Anders & Grevesse 1989 and Wilms, Allen & McCray 2000). E(B-V) values are obtained from the Harris Catalog (Harris 1996); to obtain A_V , we assumed $R_V=3.1$. Discrepancy is calculated between the measured N_H using Wilms, Allen & McCray (2000) abundances and the calculated values based on the relation of Güver & Özel (2009). All uncertainties are 90% confidence.

6266 that shows evidence for a powerlaw component (Table 4). To constrain the contribution from the powerlaw, we fixed the photon index to 1.5 due to the limited spectral quality at higher energies. We notice that there is a hint of a faint source $\sim 1''$ from CX4 (southwest of CX4, visible when the image is over-binned). To address this, we performed a second set of spectral analyses with a smaller source extraction region excluding the region of the possible nearby source, but we found no significant spectral changes suggesting the non-thermal emission is therefore intrinsic to CX4 (Table 4 contains fits performed with the standard extraction regions).

We searched for short (~ 1000 s) timescale temporal variations in each observation by performing chi-squared and KS tests, and found no evidence of variation for any of our targets in NGC 6266. No source shows probability of constancy less than 0.06% which is the 95% confidence range when considering all trials (80, for all sources in this study).

3.3 NGC 6440

NGC 6440 is a moderately extinguished GC near the Galactic center. There are at least 25 X-ray sources identified in this cluster, of which two are known transient LMXBs (NGC 6440 CX 1 = SAX J1748.9-2021, in 't Zand et al. 1999; in 't Zand et al. 2001; Pooley et al. 2002; Bozzo, Kuulkers & Ferrigno 2015; NGC 6440 X-2, Altamirano et al. 2010; Heinke et al. 2010). This cluster is 8.5 kpc away and has a reddening of $E(B-V)=1.07$ (Harris 1996). We used three long *Chandra/ACIS* observations of this cluster, obtained in 2000, 2003, and 2009. We study the four brightest identified qLMXB candidates in or near the core of this cluster, CX 1, CX 2 (not to be confused with the AMXP denoted as NGC 6440 X-2, which is not detected in deep quiescence, e.g. Heinke et al. 2010), CX 3, and CX 5, which were identified as likely qLMXBs by Pooley et al. (2002).

The *Chandra/ACIS* observation of NGC 6440 in 2009 occurred while NGC 6440 X-2 was in outburst (Heinke et al. 2010) and the image is severely piled-up in the vicinity of this source. However, we were nevertheless able to use this observation for spectral analysis of qLMXBs, as NGC 6440 X-2 is located further away from the core of the cluster ($\sim 12''$) and the outburst was relatively faint (peaking at $\sim 1 \times 10^{36}$ erg s⁻¹). We addressed the contamination from the

X-2 outburst on affected sources (CX 1, CX 2 & CX 3) by extracting background spectra from multiple regions at the same angular distance as the target from X-2. Our targets and chosen extraction regions are shown in Fig. 3.

Two of the sources in this cluster (CX 1 and CX 3) show excesses at high energies to the NSATMOS fits, so we added a powerlaw component to their spectral models. In both cases, we froze the powerlaw photon index to the value found in the best fit to all three observations. We also note that there is a hint for the presence of a very faint source near CX 3 (~ 10 times fainter than CX 3, south of it, visible when the image is over-binned), however it does not affect the spectrum. The results of our spectral analyses for NGC 6440 are tabulated in Table 5. Walsh, Cackett & Bernardini (2015) measure powerlaw contributions consistent with our results for CX 2 and CX 3 in both 2003 and 2009 observations; We note that our extraction regions might differ from the ones chosen by Walsh, Cackett & Bernardini (2015) as they do not discuss their choice of extraction regions. This is specially important due to the large and spatially varying background from the outburst of NGC 6440 X-2.

From our sample, CX 2 and CX 3 show no evidence of variation in the NS temperature. This is in general accord with the results of Walsh, Cackett & Bernardini (2015). These authors include a short (4 ks) *Chandra/ACIS* observation of NGC 6440, 12 days after our 3rd observation, and find that the flux increases in this observation for CX 5. If the spectrum is assumed to consist of only a NS atmosphere model, then the NS temperature must have increased in CX 5. However, Walsh, Cackett & Bernardini (2015) note that, since CX 5's spectrum may contain a powerlaw in this observation, the variability cannot be conclusively attributed to changes in the NS temperature. We find no evidence for variation in the spectrum of CX 5 between 2000 and 2009. We also detect the presence of a weak powerlaw component in the 2000 epoch at 1.7σ .

We found possible evidence for thermal variations in CX 1 in quiescence (Fig. 2, top right). We significantly detect a powerlaw with photon index 1.7 ± 2 in the 2000 observation, but not in the 2003 or 2009 observations. Fixing this powerlaw index to the best-fit index, our best fit finds a $-10^{+7}_{-6}\%$ change in temperature from 2000 to 2003, with the 2009 observation consistent with the 2003 observation (Table 5). This marginal evidence for variation suggests the presence of continuing accretion during the 2000 observa-

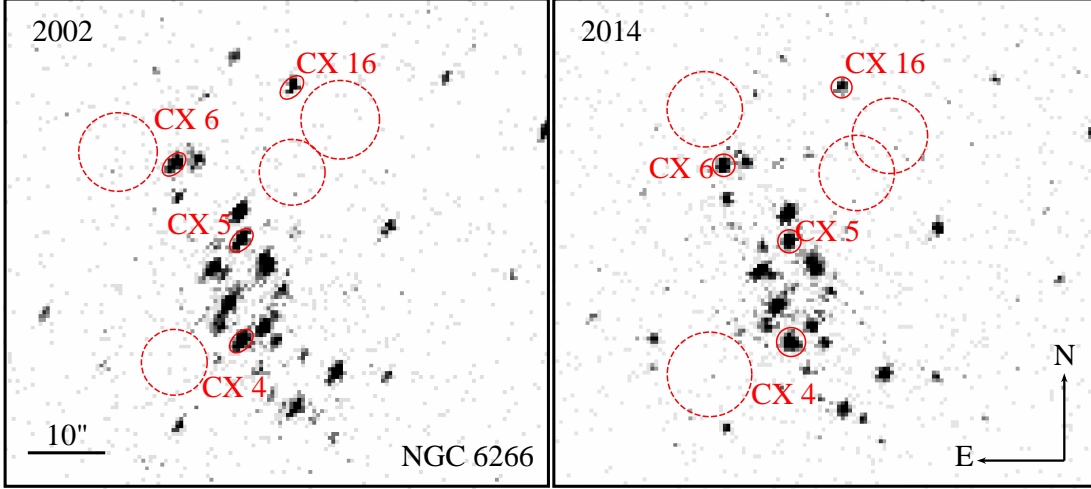


Figure 1. X-ray (0.3-7 keV) images of NGC 6266 as seen by Chandra-ACIS in 2002 (left) and 2014 (right). Source extraction regions are represented by solid circles/ellipses, and background extraction regions are represented by dashed circles. In the 2002 observation, the centre of NGC 6266 was located 2.5 arcminutes off-axis. To account for the distortion of the point-spread function this offset induced, we used elliptical extraction regions for that observation.

Source	N_H (10^{21} cm^{-2})	Year	$\log T$ (K)	% Variation	% Powerlaw flux fraction (0.5-10 keV)
NGC 6266 CX 4	3.9 ± 0.4	2002	6.057 ± 0.007	–	8 ± 7
Powerlaw $\Gamma=(1.5)$		2014	6.056 ± 0.006	< 3.2	12 ± 5
$\chi^2_\nu/\text{d.o.f} = 0.87/56$					
NGC 6266 CX 5	3.9 ± 0.4	2002	6.055 ± 0.007	–	< 9
Powerlaw $\Gamma=(1.5)$		2014	6.062 ± 0.006	< 4.7	< 7
$\chi^2_\nu/\text{d.o.f} = 0.87/52$					
NGC 6266 CX 6	4.2 ± 0.4	2002	6.056 ± 0.006	–	< 9
Powerlaw $\Gamma=(1.5)$		2014	$6.053^{+0.006}_{-0.007}$	< 3.6	< 7
$\chi^2_\nu/\text{d.o.f} = 0.64/49$					
NGC 6266 CX 16	4.3 ± 0.6	2002	5.96 ± 0.01	–	< 23
Powerlaw $\Gamma=(1.5)$		2014	5.94 ± 0.01	< 9	< 15
$\chi^2_\nu/\text{d.o.f} = 1.21/14$					

Table 4. NGC 6266: Results of spectral analysis using an absorbed NS atmosphere (TBABS*NSATMOS), plus a powerlaw added when needed. All uncertainties are 90% confidence. Temperature variations are calculated from the first observation in 2002. Powerlaw fractions are fractions of the total 0.5-10 keV flux.

tion (plausible considering that CX 1 erupted into outburst two years before, and one year after, the 2000 observation, in’t Zand et al. 2001).

Cackett et al. (2005) investigated the spectral variations of CX 1 using the first two *Chandra/ACIS* observations of NGC 6440, but they argued that the observed spectral variations were likely due to changes in the powerlaw component exclusively. Cackett et al.’s best fit uses a powerlaw component with photon index $2.5(\pm 1.0)$, which explains the difference with our best fit (photon index 1.7 ± 2); a softer powerlaw can explain flux differences in the soft X-rays, whereas our harder value of photon index require changes in the thermal component to explain. Walsh, Cackett & Bernardini (2015) also fit the spectra of CX1 in these 3 observations (adding the short 2009 obser-

vation mentioned above) using C-stats in Xspec, find a different value from Cackett et al. (2005) and basically agree with our results—the powerlaw photon index is measured at 1.6 ± 1.0 , and the 2000 data indicate a slightly higher NS temperature compared to the 2003 data, at 1σ confidence (though not at 99% confidence). Walsh et al. also conclude (from χ^2 fitting) that it is not clear whether the variation in CX1 was due exclusively to changes in the powerlaw component, exclusively to changes in the thermal component, or to changes in both. We agree with Walsh et al. that it is not clear whether the thermal component varied between the 2000 observation and later observations.

Searching for short ($\sim 1000s$) timescale variations in each observation for all sources, we found no evidence of variation. No source shows probability of constancy less than

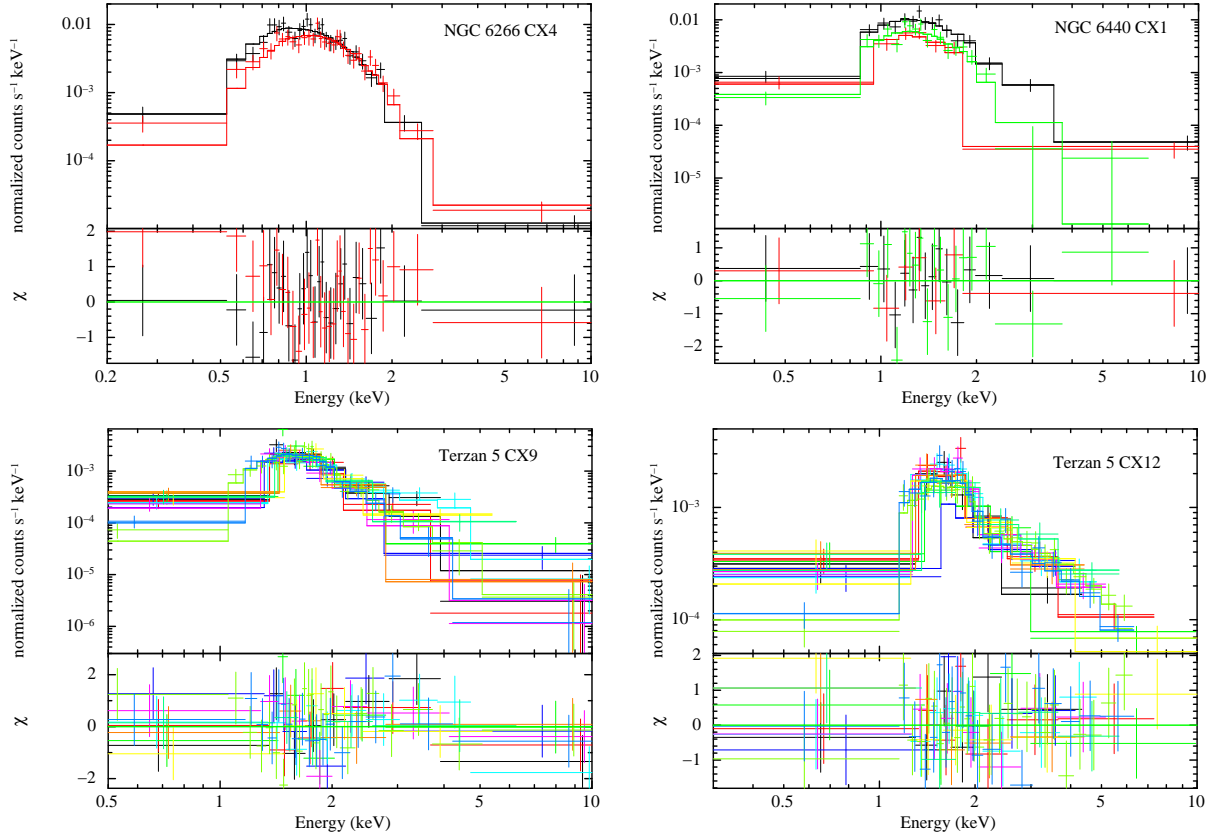


Figure 2. Examples of extracted spectra; top panels show data (crosses) and model (line). Different colours represent different epochs. Note that in addition to changes in the source, changes in the detector may alter the observed spectrum (these changes are included in the model). Top left: NGC 6266 CX4 (see §3.2). Only two *Chandra*/*ACIS* epochs are available, but the spectral quality is high. Top right: NGC 6440 CX1 (see §3.3). The black (2000) spectrum is brighter at all energies, particularly at higher energies; we attribute this to a difference in the powerlaw component, and possibly the thermal component. Bottom left & right: Terzan 5 CX9 & Terzan 5 CX12 respectively, including spectra from 11 epochs (see §3.4). The spectral fit for CX9 shown here uses a hydrogen atmosphere model. Note that there are still clear waves in the residuals (down at 2 keV, up at 3, down again at 5 keV), indicating problems with the fit (though the χ^2 is formally acceptable, 87.42 for 87 dof). These residual patterns are not completely eliminated in a helium atmosphere model, though they are reduced. CX12 shows evidence for a strong powerlaw component in this fit, as well as evidence for variation in soft X-rays (particularly in the 4th observation, taken in April 2011, colored dark blue here).

0.06% which is the 95% confidence range when considering all trials (80, for all sources in this study).

3.4 Terzan 5

Terzan 5 is a massive, highly extincted GC near the Galactic center. It is located at a distance of 5.9 ± 0.5 kpc (Valenti, Ferraro & Origlia 2007) and it harbours more than 40 X-ray sources (Heinke et al. 2006b). There are three known transient LMXBs in this cluster, the most in any Galactic GC (Bahramian et al. 2014). Terzan 5 has shown numerous outbursts (an overview up to 2012 is given in Degenaar & Wijnands 2012), several of which were not accurately localized (the most recent detected outburst without accurate localization being in 2002). It is therefore quite possible that other sources have been in outburst in the recent past.

We use all available *Chandra*/*ACIS* observations of this GC in which all sources are quiescent to study the brighter

thermally-dominated qLMXBs without observed outbursts. We start with the sample of candidate qLMXBs from Heinke et al. (2006a), which identified thermally-dominated qLMXBs by spectral fitting, or by hardness ratio plus inferred X-ray luminosity. Analyses of the quiescent behaviour of the outbursting sources Ter 5 X-1 (EXO 1745-248), X-2 (IGR J17480-2446), and X-3 (Swift J174805.3-244637) have been reported in Degenaar & Wijnands 2011; Degenaar, Brown & Wijnands 2011; Degenaar et al. 2013; Bahramian et al. 2014; Degenaar et al. 2015, so we exclude those sources here.

For the purpose of imaging and source detection, we merge all available observations following CIAO threads³. We corrected relative astrometry in all frames by matching the coordinates of 6 bright sources. We ran *reproject_aspect* to create a new reprojected aspect solution for each observation. Then we applied these aspect solutions to the event

³ <http://cxc.harvard.edu/ciao/threads/combine/>

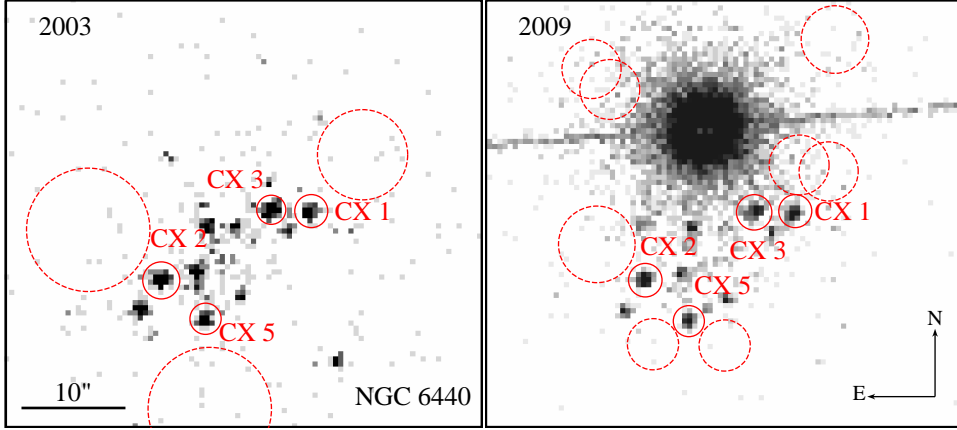


Figure 3. NGC 6440 as seen by Chandra-ACIS in the 0.3-7 keV band in 2003 (left) and 2009 (right). Solid circles represent the source extraction regions and dashed circles show the selected background regions. In the 2009 observation, the image is contaminated by an outburst from NGC 6440 X-2 (Heinke et al. 2010). We address this contamination for affected sources by choosing multiple background extraction regions at the same distance from X-2 as the target.

Source	N_H (10^{22} cm^{-2})	Year	$\log T$ (K)	% Variation	% Powerlaw flux fraction (0.5-10 keV)
NGC 6440 CX1	1.1 ± 0.1	2000	6.16 ± 0.01	10^{+7}_{-6}	26 ± 10
Powerlaw $\Gamma = (1.7)$		2003	$6.12^{+0.01}_{-0.02}$	—	< 10
$\chi^2_\nu/\text{d.o.f} = 0.84/37$		2009	6.14 ± 0.01	< 11	< 8
NGC 6440 CX2	1.1 ± 0.1	2000	6.16 ± 0.01	—	< 6
Powerlaw $\Gamma = (1.5)$		2003	6.179 ± 0.009	< 9	< 9
$\chi^2_\nu/\text{d.o.f} = 0.87/47$		2009	6.172 ± 0.007	< 7	< 7
NGC 6440 CX3	0.9 ± 0.1	2000	$6.08^{+0.02}_{-0.03}$	—	35 ± 17
Powerlaw $\Gamma = (2)$		2003	6.10 ± 0.02	< 17	33 ± 14
$\chi^2_\nu/\text{d.o.f} = 0.57/35$		2009	6.10 ± 0.02	< 17	19 ± 15
NGC 6440 CX5	1.0 ± 0.1	2000	6.09 ± 0.01	—	18 ± 15
Powerlaw $\Gamma = (1.5)$		2003	$6.10^{+0.02}_{-0.01}$	< 10	< 10
$\chi^2_\nu/\text{d.o.f} = 1.00/25$		2009	6.11 ± 0.01	< 10	< 7

Table 5. Spectral analysis of qLMXBs in NGC 6440. We fit the spectra with an absorbed NS atmosphere (TBABS*NSATMOS), and included a powerlaw component when necessary. All uncertainties are 90% confidence. Temperature variations are calculated based on the coldest measured temperature for each source. Powerlaw fractions are fractions of the total 0.5-10 keV flux. In cases where the spectral quality allows us to constrain the powerlaw photon index (CX1 and CX3), we tied the index between observations and searched for the best-fit value, then froze the index to that best-fit value; otherwise we fixed the index to 1.5. The photon index used is listed in column 1.

files by running *reproject_events*, and finally we combined the reprojected event files by running *reproject_obs*.

We selected the candidate qLMXBs which had sufficient counts for spectral analysis in each epoch (≥ 60 ; i.e. more than 4 spectral bins of 15 counts), leaving us with a sample of four thermally-dominated qLMXBs, identified as CX9, CX12, CX18, and CX21 in Heinke et al. (2006a). We used the merged image to choose source and background spectral extraction regions. This is important since in cases like CX9 and CX18, the vicinity of the source is complex and there can be multiple sources of contamination. In cases where the vicinity of the source is complex/crowded, we extracted background spectra from annuli around the targets, exclud-

ing detected sources. The combined image of Terzan 5, with our extraction regions, is presented in Fig. 4.

We combined spectra from observations which occurred less than a month apart (using *combine_spectra*), to obtain better statistics. Investigating these observations individually, no spectral variation was detected. These observations are marked in Table 1. All our targets in Terzan 5 show a high energy excess suggesting the presence of a powerlaw component in their spectra with average fraction of $\sim 10\%$ of the total flux for CX9, CX18, and CX21 and an average fraction of $\sim 33\%$ for CX 12. Comparing these with our targets in NGC 6266 and NGC 6440, where the powerlaw component is mostly detected when flux fraction is $\geq 10\%$, suggests that our detection of a powerlaw component in all

our targets in Terzan 5 might be due to the greater depth of these observations, combined with our relatively higher sensitivity to hard vs. soft photons in this heavily absorbed cluster. We froze the powerlaw photon index to 1.5 for CX9, CX18 and CX21, due to a lack of sufficient signal to constrain it. For CX12 we freeze it to the value of 1.8, obtained from the best fit to all observations.

The values of N_H for CX12, CX18 and CX21 are all in agreement with the value of $2.6 \pm 0.1 \times 10^{22} \text{ cm}^{-2}$ from previous studies (see §3.1)⁴. However, CX9 has a hydrogen column density of $3.1 \pm 0.2 \times 10^{22} \text{ cm}^{-2}$, higher than the measured value for the cluster. We investigate the high-resolution reddening map of Terzan 5 (Massari et al. 2012, available online from Cosmic-Lab⁵), and find no significant difference (<1.5%) in reddening between the direction of CX9 and the rest of the sources in our sample. This suggests that the inferred high N_H value may be caused by intrinsic absorption in the system. Spectra of CX9 are shown in Fig. 2 (bottom left).

We also performed spectral fits on CX9 by replacing the non-magnetic hydrogen atmosphere model (NSATMOS) with a non-magnetic helium atmosphere model (NSX in Xspec, Ho & Heinke 2009). This fit gives a slightly better χ^2 compared to the hydrogen atmosphere model (χ^2 decreased from 114 to 109, where both cases have 102 degrees of freedom), and also a lower absorption value of $N_H = 2.9 \pm 0.2 \times 10^{22} \text{ cm}^{-2}$, consistent with the rest of the cluster (Table 6). These results indicate that a helium atmosphere is a possible explanation for the unusual aspects of CX9's spectrum (see §4). Note that there are still clear waves in the residuals (down at 2 keV, up at 3, down again at 5 keV), indicating problems with the fit (though the χ^2 is formally acceptable, 87.42 for 87 dof). These residual patterns are not completely eliminated in a helium atmosphere model, though they are reduced.

We found no evidence regarding spectral variations between observations in CX 9, CX 18 and CX 21. However CX 12 shows marginal evidence of variation over time (Table 7). Our main fit, in which only the NS temperature and powerlaw flux are free among observations, suggests that these variations are caused by changes in the temperature of the NS, particularly a decrease in the 2011-4 epoch, and to a lesser degree in the two 2013 observations. However, the substantial powerlaw component, which is particularly strong in the epochs with the coldest NS temperature measurements, suggests that subtle changes in the powerlaw (both flux and index) might cause the variations (Fig. 2, bottom right). We note that thermal variations are only suggested in 2 epochs (2011-4 and 2013-2) out of 11. However we get an acceptable chi-squared when fitting the temperatures to a straight line. Thus we agree with Walsh, Cackett & Bernardini (2015) that these variations are not statistically significant.

⁴ In many previous studies, abundances from Anders & Grevesse (1989) have been used for absorption models. Using these abundances, Bahramian et al. (2014) find $N_H = 1.74^{+0.06}_{-0.08} \times 10^{22} \text{ cm}^{-2}$. However in the same paper they show that using Wilms, Allen & McCray (2000) abundances gives an equivalent value of $2.6 \pm 0.1 \times 10^{22} \text{ cm}^{-2}$.

⁵ <http://www.cosmic-lab.eu/tred/tred.php>

Terzan 5 CX9			
Parameter	Hydrogen		Helium
	Trial 1	Trial 2	Trial 3
N_H (10^{22} cm^{-2})	3.1 ± 0.2	(2.6)	2.9 ± 0.2
logT (K)	6.12 ± 0.01	6.21 ± 0.06	6.10 ± 0.01
NS R (km)	(10)	7 ± 1	(10)
PL flux ^A	1.1 ± 0.3	1.3 ± 0.3	0.9 ± 0.3
$\chi^2_{\nu}/\text{d.o.f}$	1.11/102	1.24/102	1.07/102
NHP	0.20	0.05	0.29

Table 6. Tests of hydrogen (NSATMOS) and helium (NSX) atmosphere models for Terzan 5 CX9. Two trials use hydrogen atmospheres: in trial 1, N_H is free, while the NS radius is fixed to 10 km. In trial 2, N_H is fixed to the average value for Terzan 5, and the NS radius is free. Trial 3 is the same as trial 1, except using a helium atmosphere. Since we didn't find any sign of variation in our initial fits, all values are tied between epochs. The neutron star mass is assumed to be $1.4 M_{\odot}$ in each case. Uncertainties are 90% confidence, and values in parentheses are frozen. ^A: power-law fluxes are in units of $10^{-14} \text{ erg s}^{-1} \text{ cm}^{-2}$, in the 0.5-10 keV range. NHP is null hypothesis probability.

To investigate the origin of CX12's spectral variations more carefully, we perform fits letting different pairs of model parameters vary; kT and PL flux (Fit 1), N_H and PL flux (Fit 2), or PL Γ and PL flux (Fit 3; see Table 8). In fit 1, variations in both kT and the PL flux are seen, and the fit is reasonable. However, the variations in kT appear to be anticorrelated with the variations in PL flux, which is unlike, for instance, the behaviour of Cen X-4 (Cackett et al. 2010). It should be noted that the signature of variation comes mainly from two data points (epochs 2011/4 and 2013/2). Performing a chi-squared test of constancy on temperature measured in all epochs gives a null hypothesis probability of 0.55, providing little evidence for variation. Compared to fit 1, fit 3 shows an increase of 14 in χ^2 (107 compared to 93, both fits have 96 degrees of freedom, giving a relative likelihood of 9×10^{-4} for fit 3 compared to fit 1 based on Akaike information criterion), indicating that changes in the powerlaw alone (both index and flux) are insufficient to drive the variations. However, fit 2, varying N_H and PL flux, gave a similar fit quality to fit 1 ($\chi^2 = 92.6$ compared to $\chi^2 = 93.4$, both with 96 degrees of freedom). Thus, the variations may plausibly be caused by changes in the NS temperature, or changes in intrinsic absorption, along with changes in the PL flux. Since we do not have independent evidence of the inclination of CX12, it is quite possible that this system is nearly edge-on, and that we suffer varying obscuration levels at different times.

We performed chi-squared and KS tests on individual lightcurves extracted from each observation for our target sources (excluding observation 13705, due to its short exposure). We found evidence of short (~ 1000 s) timescale variations in Terzan 5 CX 21's lightcurve, in observation 14475 (Sept. 2012, Fig. 5). A KS test gives probability of constancy $= 4.6 \times 10^{-4}$ for this lightcurve, which is slightly higher than 95% confidence, when accounting for the number of trials (80, for all sources in this study). Note that although there is evidence for presence of the PL in this epoch, the PL flux fraction is rather small ($13^{+16}_{-11} \%$), suggesting that the ther-

mal fraction is also likely to vary. It is also possible that variations observed for this source are due to eclipse in the system, however we do not find evidence for eclipse in other epochs. No other source shows KS probability of constancy less than 0.06% (95% confidence).

4 DISCUSSION

4.1 Terzan 5 CX9: a NS with a helium atmosphere?

Terzan 5 CX 9 shows an unusual spectral shape compared to other *q*LMXBs, with significantly lower flux at low energies (between 0.1 and 1 keV), compared to similar sources. This could be due to a higher amount of absorption. Investigating the reddening map of this cluster, we can rule out differential reddening. However, there could be additional intrinsic absorption, for instance if we are looking at the system edge-on.

Another possibility is that this NS may have an atmosphere composed of helium. Ultracompact X-ray binaries (with a white dwarf donor star, possessing no hydrogen) are fairly common among bright LMXBs in globular clusters (e.g. Zurek et al. 2009). Helium white dwarf donors might thus be expected to lead to helium atmospheres on the NSs; there is evidence for low hydrogen content in X-ray bursts from some bright ultracompact X-ray binaries (Cumming 2003; Galloway et al. 2008). The X-ray spectra of helium atmospheres are similar to hydrogen atmospheres, but slightly harder (Romani 1987; Ho & Heinke 2009). An observed spectrum will thus give different parameter values for He vs. H atmospheres, and several papers have considered the importance of atmosphere composition for attempts to constrain the NS mass and radius (Servillat et al. 2012; Catuneanu et al. 2013; Lattimer & Steiner 2014; Heinke et al. 2014). For relatively low-count spectra such as CX9, which parameter is different from other NS *q*LMXBs—e.g., atmospheric composition (H or He), vs. N_H —may not be possible to differentiate. No helium atmosphere has yet been confidently identified on a NS, so any evidence in favor of a helium atmosphere is intriguing.

4.2 Possible continuous accretion for NGC 6440 CX1 & Terzan 5 CX12

NGC 6440 CX 1 is the brightest X-ray source in the cluster. It has shown multiple X-ray outbursts over the last 20 years (1998, 2001, 2005, 2010, 2015; in 't Zand et al. 1999; in 't Zand et al. 2001; Markwardt & Swank 2005; Patruno et al. 2010; Homan, Pooley & Heinke 2015). In quiescence, it shows a mostly thermal spectrum although there are signs of variations in the spectrum over the course of years. In the 2000 observation, we find that the spectrum requires a powerlaw component for a good fit, but in later observations this component is not required. Cackett et al. (2005) argued that the changing normalization of the powerlaw component, with photon index ~ 2.5 , was the main source of spectral variation. However, we suggest that the unusually high photon index used there led to the overestimation of

the powerlaw's contribution. Walsh, Cackett & Bernardini (2015) also fit the spectra of CX 1 with similar models. They find that formally, either the powerlaw or thermal component can be the source of variation, and we agree with that finding. However, when we hold the NS temperature constant across the epochs while allowing the powerlaw normalization to vary (with photon index tied to a single value across epochs), the best-fit value of the powerlaw photon index will increase to 2.7 ± 0.5 (compared to 1.7 ± 2 when the NS temperature also varies). This agrees with Walsh et al.'s fit results when assuming NS temperature fixed (the first fit in their Table 4), where they find a photon index of 3.1 ± 0.5 . The anomalously high photon index required for such a fit strongly argues that the thermal component may also be varying.

Terzan 5 CX12 is well-fit by an absorbed two-component (thermal+powerlaw) model, with an N_H column typical of sources in the cluster ($2.6 \pm 0.1 \times 10^{22} \text{ cm}^{-2}$). CX12 shows hints of spectral variations, concentrated at low energies (< 2 keV; see Figure 2, lower right). Thus it's unlikely that the powerlaw component is responsible for these variations. Intrinsic absorption (e.g. an edge-on system, where an uneven accretion disk occasionally blocks the line of sight), or continuing thermal variation due to accretion are possible origins of these variations.

4.3 Variability of thermal component in *q*LMXBs

In our sample of 12 globular cluster *q*LMXBs, NGC 6440 CX1 and Terzan 5 CX12 are the only sources that show evidence of variations in the thermal component over timescales of years. In both cases, the thermal component appears to be the most plausible origin of the variations, but in neither case can thermal variations be proven. For NGC 6440 CX1, the best-fit thermal variation is only a 10% temperature change, while for Terzan 5 CX12 one observation appears to have a 20% drop.

Terzan 5 CX 21 shows evidence of variability on timescales of hours (within observations), although we did not detect variations on longer timescales (between observations). This variability may be due to variations in the (dominant) thermal component in quiescence. Alternatively, it may be caused by eclipses by the companion, if the system is at a high inclination angle.

A crucial result of our analysis is that we have assembled an additional 7 *q*LMXBs (in addition to 4 others previously reported, see Introduction) with multiple high-quality X-ray spectra showing little or no evidence for a powerlaw component; NGC 6266 CX4, CX5, CX6, and CX16, and NGC 6440 CX1 (considering only the 2003 and 2009 observations), CX2, and CX5. None of these objects show evidence for a powerlaw component comprising more than 12% of the 0.5-10 keV flux (except for the 2000 observation of CX1, which we exclude here). The upper limits on a powerlaw (assuming a photon index of 1.5) are, in four cases, $< 10\%$ of the 0.5-10 keV flux, and $< 17\%$ or $< 23\%$ in two others. Using *Chandra* observations spaced over 9-12 years (6 for NGC 6440 CX1), we can constrain the thermal emission from these NS to not have varied by more than 10% in any of these sources. Combined with the literature con-

Source	Epoch	logT (K)	% Variation	% Powerlaw flux fraction (0.5-10 keV)
Terzan 5 CX 9	2003	$6.13^{+0.01}_{-0.02}$	<15	7^{+7}_{-6}
Powerlaw $\Gamma=1.5$	2009	6.11 ± 0.02	<12	<14
$N_H = 3.1 \pm 0.2 \times 10^{22}$	2011-2	6.12 ± 0.02	<15	12^{+10}_{-8}
$\chi^2_{\nu}/\text{d.o.f} = 1.00/87$	2011-4	6.11 ± 0.02	<12	8^{+9}_{-7}
	2011-9	6.10 ± 0.02	–	22^{+11}_{-9}
	2012-5	$6.12^{+0.01}_{-0.02}$	<12	<8
	2012-9	6.11 ± 0.02	<12	11^{+10}_{-8}
	2012-10	6.13 ± 0.02	<17	<8
	2013-2	$6.125^{+0.007}_{-0.008}$	<13	4^{+3}_{-2}
	2013-7	6.12 ± 0.02	<15	10^{+10}_{-8}
	2014	$6.128^{+0.008}_{-0.009}$	<14	<5
Terzan 5 CX 12	2003	6.09 ± 0.02	23^{+31}_{-16}	14^{+10}_{-8}
Powerlaw $\Gamma=1.8\pm0.3$	2009	$6.08^{+0.02}_{-0.03}$	20^{+31}_{-18}	27^{+13}_{-10}
$N_H = 2.6 \pm 0.2 \times 10^{22}$	2011-2	$6.07^{+0.02}_{-0.03}$	<48	29^{+16}_{-13}
$\chi^2_{\nu}/\text{d.o.f} = 0.97/96$	2011-4	$6.00^{+0.04}_{-0.08}$	–	52^{+27}_{-18}
	2011-9	$6.09^{+0.02}_{-0.03}$	23^{+32}_{-18}	28^{+11}_{-9}
	2012-5	$6.09^{+0.02}_{-0.02}$	23^{+32}_{-16}	27^{+11}_{-9}
	2012-9	$6.07^{+0.03}_{-0.04}$	<51	34^{+17}_{-13}
	2012-10	$6.08^{+0.02}_{-0.03}$	20^{+31}_{-18}	29^{+16}_{-13}
	2013-2	$6.04^{+0.02}_{-0.02}$	<38	44^{+8}_{-7}
	2013-7	$6.05^{+0.03}_{-0.06}$	<44	49^{+22}_{-16}
	2014	$6.07^{+0.02}_{-0.01}$	17^{+31}_{-12}	29^{+7}_{-6}
Terzan 5 CX 18	2003	6.09 ± 0.02	<17	13^{+11}_{-8}
Powerlaw $\Gamma=1.5$	2009	6.09 ± 0.02	<17	<13
$N_H = 2.7 \pm 0.2 \times 10^{22}$	2011-2	6.10 ± 0.02	<20	<7
$\chi^2_{\nu}/\text{d.o.f} = 1.12/51$	2011-4	6.08 ± 0.02	<15	<14
	2011-9	6.08 ± 0.02	<15	7^{+8}_{-6}
	2012-5	6.07 ± 0.02	<12	7^{+9}_{-7}
	2012-9	$6.07^{+0.02}_{-0.03}$	–	<13
	2012-10	$6.09^{+0.02}_{-0.03}$	<17	<13
	2013-2	6.08 ± 0.01	<12	12 ± 1
	2013-7	$6.07^{+0.02}_{-0.03}$	<12	10^{+14}_{-10}
	2014	6.09 ± 0.01	<15	7 ± 1
Terzan 5 CX 21	2003	$6.04^{+0.02}_{-0.03}$	<15	16^{+16}_{-12}
Powerlaw $\Gamma=1.5$	2009	$6.06^{+0.02}_{-0.03}$	<20	10^{+12}_{-9}
$N_H = 2.4 \pm 0.2 \times 10^{22}$	2011-2	$6.07^{+0.02}_{-0.03}$	<23	<12
$\chi^2_{\nu}/\text{d.o.f} = 0.92/36$	2011-4	6.03 ± 0.03	–	17^{+16}_{-11}
	2011-9	6.08 ± 0.02	<26	<10
	2012-5	6.04 ± 0.02	<15	<15
	2012-9	$6.04^{+0.02}_{-0.04}$	<15	13^{+16}_{-11}
	2012-10	$6.05^{+0.02}_{-0.03}$	<17	11^{+14}_{-10}
	2013-2	6.04 ± 0.01	<12	11^{+5}_{-4}
	2013-7	6.06 ± 0.02	<20	<7
	2014	6.05 ± 0.01	<15	<16

Table 7. Spectral analyses of Terzan 5 targets with an absorbed NS atmosphere + powerlaw. All uncertainties are 90% confidence. Temperature variations are calculated based on the coldest measured temperature for each source. The “Epoch” values give the year and month, in cases where multiple observations per year were performed. Powerlaw fractions are fractions of the total unabsorbed 0.5-10 keV flux. All targets in Terzan 5 show significant evidence for the presence of a powerlaw component in their spectrum. In cases where the spectral quality allows us to constrain the powerlaw photon index (CX 12), we tied the index between observations and searched for the best-fit value, then froze the index to that best-fit value; otherwise we fixed the index to 1.5. The photon index used is listed in column 1. N_H values are in units of cm^{-2} .

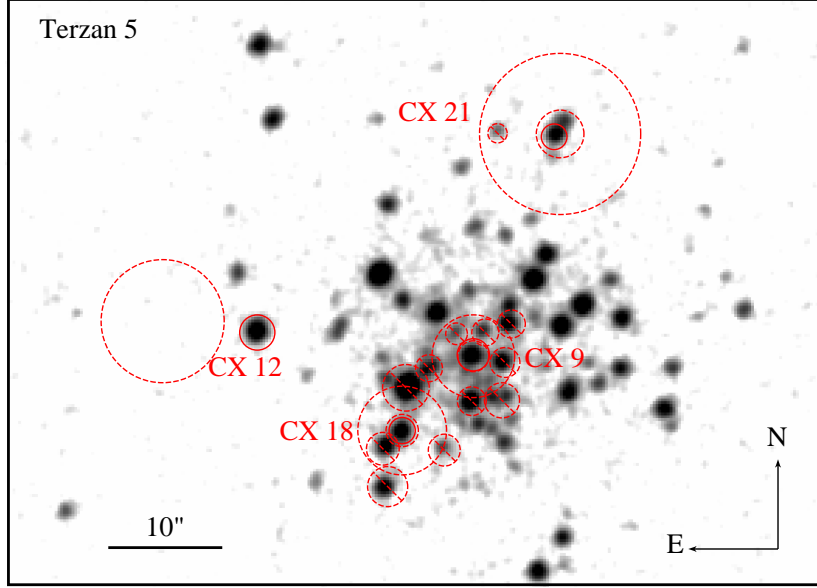


Figure 4. Stacked and smoothed *Chandra*/*ACIS* image of Terzan 5 in 0.3-7 keV band (total ~ 620 ks). Source extraction regions for our targets are shown with red solid circles, and regions for background regions are represented by dashed circles/annuli. For targets in complex regions, we extracted background from annuli. Dashed circles with slashes represent excluded regions in background extraction (i.e. contaminating sources).

Terzan 5 CX12						
Epoche	Fit 1		Fit 2		Fit 3	
	Constant N_H & Γ		Constant T_{NS} & Γ		Constant N_H & T_{NS}	
	$\log T$ (K)	PL flux ($10^{-14}\text{erg s}^{-1} \text{ cm}^{-2}$)	N_H (10^{22}cm^{-2})	PL flux ($10^{-14}\text{erg s}^{-1} \text{ cm}^{-2}$)	Γ	PL flux ($10^{-14}\text{erg s}^{-1} \text{ cm}^{-2}$)
2003	6.09±0.02	2±1	2.5 ^{+0.3} _{-0.2}	2±1	3.1 ^{+0.8} _{-0.7}	7 ⁺⁶ ₋₃
2009	6.08 ^{+0.02} _{-0.03}	5±2	2.5 ^{+0.3} _{-0.2}	5±1	2.4±0.7	7 ⁺⁴ ₋₂
2011-2	6.07 ^{+0.02} _{-0.03}	4±2	2.7 ^{+0.5} _{-0.3}	4±2	2.3±0.7	6 ⁺³ ₋₂
2011-4	6.00 ^{+0.04} _{-0.08}	6±2	3.5 ^{+0.6} _{-0.4}	5±2	1.3 ^{+0.6} _{-0.7}	4±1
2011-9	6.09 ^{+0.02} _{-0.03}	5±2	2.5 ^{+0.3} _{-0.2}	5±1	2.4±0.6	8 ⁺³ ₋₂
2012-5	6.09 ^{+0.02} _{-0.02}	5±1	2.4 ^{+0.3} _{-0.2}	5±1	2.4±0.6	8 ⁺⁴ ₋₂
2012-9	6.07 ^{+0.03} _{-0.04}	6±2	2.5 ^{+0.5} _{-0.3}	5±2	1.8±0.8	6 ⁺³ ₋₂
2012-10	6.08 ^{+0.02} _{-0.03}	5±2	2.3 ^{+0.4} _{-0.3}	5±2	2±1	7 ⁺⁵ ₋₂
2013-2	6.04 ^{+0.02} _{-0.02}	7±2	3.0 ^{+0.3} _{-0.2}	6±1	1.6±0.3	6±1
2013-7	6.05 ^{+0.03} _{-0.06}	8±2	2.8 ^{+0.6} _{-0.4}	8±2	1.8±0.5	8±2
2014	6.07 ^{+0.02} _{-0.01}	5±1	2.6 ^{+0.2} _{-0.2}	5±1	2.2±0.4	6±1
$\chi^2_\nu/\text{d.o.f}$	0.97/96		0.96/96		1.12/96	
NHP	0.55		0.58		0.20	

Table 8. Testing three possibilities to explain the spectral variations in Terzan 5 CX12. Fit 1: Fixing N_H and the powerlaw photon index to their best-fit value across all spectra ($N_H = 2.6 \times 10^{22} \text{ cm}^{-2}$, $\Gamma = 1.8$), while letting the NS temperature and powerlaw flux vary between epochs. Fit 2: Allowing N_H and powerlaw flux to vary across epochs, while fixing the NS temperature and powerlaw photon-index ($\log T = 6.08$, $\Gamma = 1.7$). Fit 3: Only photon index and powerlaw flux are allowed to vary between epochs, with N_H and the NS temperature frozen ($N_H = 2.5 \times 10^{22} \text{ cm}^{-2}$, $\log T = 6.05$). powerlaw fluxes are given in 0.5-10 keV band. The NS mass and radius are frozen to their canonical values of $1.4 M_\odot$ and 10 km in all cases. All uncertainties are 90% confidence. NHP is null hypothesis probability.

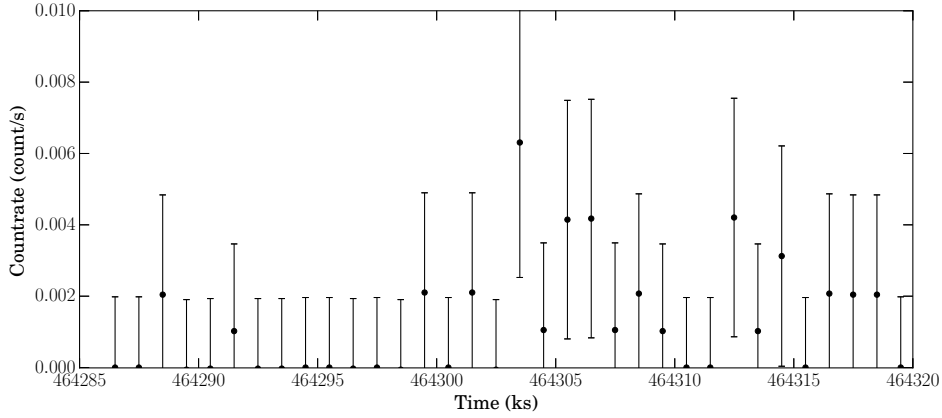


Figure 5. Binned lightcurve of Terzan 5 CX 21 from observation 14475 (Sept. 2012). A KS test gives probability of constancy = 4.6×10^{-4} for this lightcurve, which is slightly higher than 95% confidence, when accounting for the number of trials. It is possible that this variation may be due to eclipse. However we do not find strong evidence for eclipse in other epochs of this source.

straints on 4 other sources discussed in §1 (and in agreement with the recent work of Walsh, Cackett & Bernardini 2015), this provides increasing evidence that the thermal X-ray spectral components of NS qLMXBs without powerlaw components to their spectra are not powered by continuing accretion. (Of course, a clear detection of intrinsic variation of the thermal component in a source without a powerlaw component would disprove this hypothesis.) This contrasts with recent works that indicate that in some NS qLMXBs with powerlaw components, the powerlaw, as well as some of the thermal component, is powered by continuing, variable, accretion onto the NS surface (Cackett et al. 2010; Bahramian et al. 2014; Chakrabarty et al. 2014; D’Angelo et al. 2015; Wijnands et al. 2014).

This evidence against continuing accretion for those qLMXBs without powerlaw components also supports the use of these qLMXB spectra to obtain constraints on the mass and radius (and thus on the equation of state) of NSs, since a lack of accretion indicates that the atmosphere will not be contaminated by heavy elements.

ACKNOWLEDGMENTS

This research has made use of the following data and software packages: observations made by the Chandra X-ray Observatory, data obtained from the Chandra Data Archive, software provided by the Chandra X-ray Center (CXC) in the application package CIAO, and software provided by the High Energy Astrophysics Science Archive Research Center in the HEASOFT package. We acknowledge extensive use of the ADS and arXiv. AB thanks G.R.Sivakoff and T.J.Maccarone for helpful discussions. COH acknowledges financial support from NSERC Discovery Grants, an Alberta Ingenuity New Faculty Award, and an Alexander von Humboldt Fellowship. ND acknowledges support via an EU Marie Curie Intra-European fellowship under contract no. FP-PEOPLE-2013-IEF-627148. LC acknowledges support from a *Chandra* grant associated with Obs.ID #15761.

WCGH acknowledges support from STFC in the UK. This work was partially supported by the NSF through grant AST-1308124.

REFERENCES

- Altamirano D., Patruno A., Markwardt C. B., et al., 2010, *ApJL*, 712, L58
- Anders E., Grevesse N., 1989, *GCA*, 53, 197
- Archibald A. M. et al., 2014, *ArXiv e-prints*, arXiv:1412.1306
- Arnaud K. A., 1996, in *ASP Conf. Ser. 101: Astronomical Data Analysis Software and Systems V*, p. 17
- Bahramian A. et al., 2014, *ApJ*, 780, 127
- Balucinska-Church M., McCammon D., 1992, *ApJ*, 400, 699
- Bogdanov S., Grindlay J. E., van den Berg M., 2005, *ApJ*, 630, 1029
- Bozzo E., Kuulkers E., Ferrigno C., 2015, *The Astronomer’s Telegram*, 7106, 1
- Brown E. F., Bildsten L., Chang P., 2002, *ApJ*, 574, 920
- Brown E. F., Bildsten L., Rutledge R. E., 1998, *ApJL*, 504, L95
- Cackett E. M., Brown E. F., Miller J. M., Wijnands R., 2010, *ApJ*, 720, 1325
- Cackett E. M., Fridriksson J. K., Homan J., Miller J. M., Wijnands R., 2011, *MNRAS*, 414, 3006
- Cackett E. M. et al., 2005, *ApJ*, 620, 922
- Cackett E. M., Wijnands R., Miller J. M., Brown E. F., Degenaar N., 2008, *ApJL*, 687, L87
- Campana S., Colpi M., Mereghetti S., Stella L., Tavani M., 1998, *A&A Rev.*, 8, 279
- Campana S., Israel G. L., Stella L., Gastaldello F., Mereghetti S., 2004, *ApJ*, 601, 474
- Campana S., Mereghetti S., Stella L., Colpi M., 1997, *A&A*, 324, 941
- Campana S., Stella L., 2003, *ApJ*, 597, 474

- Catuneanu A., Heinke C. O., Sivakoff G. R., Ho W. C. G., Servillat M., 2013, *ApJ*, 764, 145
- Chakrabarty D. et al., 2014, *ApJ*, 797, 92
- Chang P., Bildsten L., 2004, *ApJ*, 605, 830
- Chomiuk L., Strader J., Maccarone T. J., Miller-Jones J. C. A., Heinke C., Noyola E., Seth A. C., Ransom S., 2013, *ApJ*, 777, 69
- Clark G. W., 1975, *ApJL*, 199, L143
- Colpi M., Geppert U., Page D., Possenti A., 2001, *ApJL*, 548, L175
- Cumming A., 2003, *ApJ*, 595, 1077
- D’Angelo C. R., Fridriksson J. K., Messenger C., Patruno A., 2015, *MNRAS*, 449, 2803
- D’Angelo C. R., Spruit H. C., 2010, *MNRAS*, 406, 1208
- D’Angelo C. R., Spruit H. C., 2012, *MNRAS*, 420, 416
- Degenaar N., Brown E. F., Wijnands R., 2011, *MNRAS*, 418, L152
- Degenaar N., Wijnands R., 2011, *MNRAS*, 412, L68
- Degenaar N., Wijnands R., 2012, *MNRAS*, 422, 581
- Degenaar N. et al., 2015, *MNRAS*, 451, 2071
- Degenaar N. et al., 2013, *ApJ*, 775, 48
- Degenaar N. et al., 2011, *MNRAS*, 412, 1409
- Deufel B., Dullemond C. P., Spruit H. C., 2001, *A&A*, 377, 955
- Foight D., Guver T., Ozel F., Slane P., 2015, *ArXiv e-prints*, arXiv:1504.07274
- Fridriksson J. K. et al., 2011, *ApJ*, 736, 162
- Fridriksson J. K. et al., 2010, *ApJ*, 714, 270
- Fruscione A., McDowell J. C., Allen G. E., Brickhouse N. S., et al., 2006, in *Society of Photo-Optical Instrumentation Engineers (SPIE) Conference Series*, Vol. 6270, Society of Photo-Optical Instrumentation Engineers (SPIE) Conference Series
- Galloway D. K., Muno M. P., Hartman J. M., Psaltis D., Chakrabarty D., 2008, *ApJ Supp*, 179, 360
- Grindlay J. E., Heinke C., Edmonds P. D., Murray S. S., 2001, *Science*, 292, 2290
- Guillot S., Rutledge R. E., 2014, *ApJL*, 796, L3
- Guillot S., Rutledge R. E., Brown E. F., 2011, *ApJ*, 732, 88
- Guillot S., Servillat M., Webb N. A., Rutledge R. E., 2013, *ApJ*, 772, 7
- Güver T., Özel F., 2009, *MNRAS*, 400, 2050
- Harris W. E., 1996, *AJ*, 112, 1487
- Heinke C. O., Altamirano D., Cohn H. N., et al., 2010, *ApJ*, 714, 894
- Heinke C. O. et al., 2014, *MNRAS*, 444, 443
- Heinke C. O., Edmonds P. D., Grindlay J. E., Lloyd D. A., Cohn H. N., Lugger P. M., 2003a, *ApJ*, 590, 809
- Heinke C. O., Grindlay J. E., Edmonds P. D., 2005, *ApJ*, 622, 556
- Heinke C. O., Grindlay J. E., Edmonds P. D., Lloyd D. A., Murray S. S., Cohn H. N., Lugger P. M., 2003b, *ApJ*, 598, 516
- Heinke C. O., Grindlay J. E., Lloyd D. A., Edmonds P. D., 2003c, *ApJ*, 588, 452
- Heinke C. O., Grindlay J. E., Lugger P. M., Cohn H. N., Edmonds P. D., Lloyd D. A., Cool A. M., 2003d, *ApJ*, 598, 501
- Heinke C. O., Jonker P. G., Wijnands R., Deloye C. J., Taam R. E., 2009, *ApJ*, 691, 1035
- Heinke C. O., Rybicki G. B., Narayan R., Grindlay J. E., 2006a, *ApJ*, 644, 1090
- Heinke C. O., Wijnands R., Cohn H. N., Lugger P. M., Grindlay J. E., Pooley D., Lewin W. H. G., 2006b, *ApJ*, 651, 1098
- Ho W. C. G., Heinke C. O., 2009, *Natur*, 462, 71
- Homan J., Fridriksson J. K., Wijnands R., Cackett E. M., Degenaar N., Linares M., Lin D., Remillard R. A., 2014, *ApJ*, 795, 131
- Homan J., Pooley D., Heinke C., 2015, *The Astronomer’s Telegram*, 7183, 1
- Illarionov A. F., Sunyaev R. A., 1975, *A&A*, 39, 185
- in ’t Zand J. J. M., Verbunt F., Strohmayer T. E., et al., 1999, *A&A*, 345, 100
- in’t Zand J. J. M., van Kerkwijk M. H., Pooley D., Verbunt F., Wijnands R., Lewin W. H. G., 2001, *ApJL*, 563, L41
- Jonker P. G., Galloway D. K., McClintock J. E., Buxton M., Garcia M., Murray S., 2004, *MNRAS*, 354, 666
- Katz J. I., 1975, *Natur*, 253, 698
- Kulkarni A. K., Romanova M. M., 2008, *MNRAS*, 386, 673
- Lattimer J. M., Steiner A. W., 2014, *ApJ*, 784, 123
- Linares M. et al., 2014, *MNRAS*, 438, 251
- Markwardt C. B., Swank J. H., 2005, *The Astronomer’s Telegram*, 495, 1
- Massari D. et al., 2012, *ApJL*, 755, L32
- Maxwell J. E., Lugger P. M., Cohn H. N., Heinke C. O., Grindlay J. E., Budac S. A., Drukier G. A., Bailyn C. D., 2012, *ApJ*, 756, 147
- Miller J. M., Cackett E. M., Reis R. C., 2009, *ApJL*, 707, L77
- Miller J. M. et al., 2013, *ApJL*, 779, L2
- Negueruela I., Reig P., Finger M. H., Roche P., 2000, *A&A*, 356, 1003
- Nowak M. A., Heinz S., Begelman M. C., 2002, *ApJ*, 573, 778
- Ozel F., Psaltis D., Guver T., Baym G., Heinke C., Guillot S., 2015, *ArXiv e-prints*, arXiv:1505.05155
- Papitto A., de Martino D., Belloni T. M., Burgay M., Pelizzoni A., Possenti A., Torres D. F., 2015, *MNRAS*, 449, L26
- Patruno A., Altamirano D., Watts A., et al., 2010, *The Astronomer’s Telegram*, 2407, 1
- Pooley D., Hut P., 2006, *ApJL*, 646, L143
- Pooley D., Lewin W. H. G., Anderson S. F., et al., 2003, *ApJL*, 591, L131
- Pooley D., Lewin W. H. G., Verbunt F., et al., 2002, *ApJ*, 573, 184
- Predehl P., Costantini E., Hasinger G., Tanaka Y., 2003, *Astronomische Nachrichten*, 324, 73
- Rajagopal M., Romani R. W., 1996, *ApJ*, 461, 327
- Reig P., Doroshenko V., Zezas A., 2014, *MNRAS*, 445, 1314
- Romani R. W., 1987, *ApJ*, 313, 718
- Romanova M. M., Ustyugova G. V., Koldoba A. V., Lovelace R. V. E., 2002, *ApJ*, 578, 420
- Rutledge R. E., Bildsten L., Brown E. F., Pavlov G. G., Zavlin V. E., 1999, *ApJ*, 514, 945
- Rutledge R. E., Bildsten L., Brown E. F., Pavlov G. G., Zavlin V. E., 2001, *ApJ*, 551, 921
- Rutledge R. E., Bildsten L., Brown E. F., Pavlov G. G.,

- Zavlin V. E., 2002a, *ApJ*, 578, 405
- Rutledge R. E., Bildsten L., Brown E. F., Pavlov G. G.,
Zavlin V. E., 2002b, *ApJ*, 577, 346
- Rutledge R. E., Bildsten L., Brown E. F., Pavlov G. G.,
Zavlin V. E., Ushomirsky G., 2002c, *ApJ*, 580, 413
- Servillat M., Heinke C. O., Ho W. C. G., Grindlay J. E.,
Hong J., van den Berg M., Bogdanov S., 2012, *MNRAS*,
423, 1556
- Steiner A. W., Lattimer J. M., Brown E. F., 2010, *ApJ*,
722, 33
- Steiner A. W., Lattimer J. M., Brown E. F., 2013, *ApJL*,
765, L5
- Ushomirsky G., Rutledge R. E., 2001, *MNRAS*, 325, 1157
- Valenti E., Ferraro F. R., Origlia L., 2007, *AJ*, 133, 1287
- Verner D. A., Ferland G. J., Korista K. T., Yakovlev D. G.,
1996, *ApJ*, 465, 487
- Walsh A. R., Cackett E. M., Bernardini F., 2015, *MNRAS*,
449, 1238
- Webb N. A., Barret D., 2007, *ApJ*, 671, 727
- Wijnands R., Degenaar N., Armas Padilla M., Altamirano
D., Cavecchi Y., Linares M., Bahramian A., Heinke C. O.,
2014, *ArXiv e-prints*, arXiv:1409.6265
- Wijnands R., Degenaar N., Page D., 2013, *MNRAS*, 432,
2366
- Wijnands R., Guainazzi M., van der Klis M., Méndez M.,
2002, *ApJL*, 573, L45
- Wijnands R., Heinke C. O., Pooley D., Edmonds P. D.,
Lewin W. H. G., Grindlay J. E., Jonker P. G., Miller J. M.,
2005, *ApJ*, 618, 883
- Wijnands R., Nowak M., Miller J. M., Homan J., Wachter
S., Lewin W. H. G., 2003, *ApJ*, 594, 952
- Wilms J., Allen A., McCray R., 2000, *ApJ*, 542, 914
- Zampieri L., Turolla R., Zane S., Treves A., 1995, *ApJ*,
439, 849
- Zane S., Turolla R., Treves A., 2000, *ApJ*, 537, 387
- Zavlin V. E., Pavlov G. G., Shibanov Y. A., 1996, *A&A*,
315, 141
- Zurek D. R., Knigge C., Maccarone T. J., Dieball A., Long
K. S., 2009, *ApJ*, 699, 1113

This paper has been typeset from a \LaTeX file prepared by the author.